

See discussions, stats, and author profiles for this publication at: <https://www.researchgate.net/publication/231663501>

Ring-Opening Reaction of Cyclobutene Radical Cation: Effect of Solvent on Competing Pathways

ARTICLE *in* THE JOURNAL OF PHYSICAL CHEMISTRY A · DECEMBER 1998

Impact Factor: 2.69 · DOI: 10.1021/jp983720p

CITATIONS

19

READS

10

4 AUTHORS, INCLUDING:



Vincenzo Barone

Scuola Normale Superiore di Pisa

772 PUBLICATIONS 43,620 CITATIONS

SEE PROFILE



G Narahari Sastry

Indian Institute of Chemical Technology

262 PUBLICATIONS 5,214 CITATIONS

SEE PROFILE

Ring-Opening Reaction of Cyclobutene Radical Cation: Effect of Solvent on Competing Pathways

Vincenzo Barone,^{*,†} Nadia Rega,[‡] Thomas Bally,^{*,‡} and G. Narahari Sastry^{*,§}

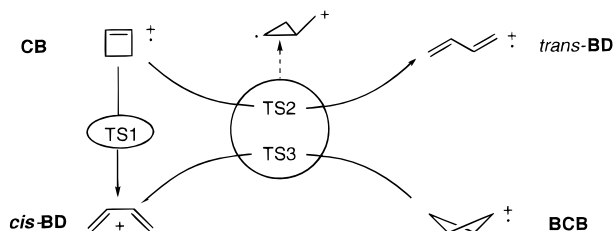
Dipartimento di Chimica, Università Federico II, via Mezzocannone 4, I-80134 Napoli, Italy, and
Institute of Physical Chemistry, The University of Fribourg, CH-1700, Fribourg, Switzerland

Received: September 15, 1998; In Final Form: November 12, 1998

We have recomputed the activation barriers for the different modes of ring opening of the cyclobutene radical cation (see: Sastry, G. N.; Bally, T.; Hroudá, V.; Carsky, P. *J. Am. Chem. Soc.* **1998**, *120*, 9323) in CHCl_3 , a typical solvent for studies of radical cation reactions, by a polarizable continuum model. Thereby, we found a clear preference for the reaction leading directly to *trans*-butadiene radical cation via a cyclopropenyl–carbinyl type radical cation, in contrast to expectations of a normal “electrocyclic” pathway leading to *cis*-butadiene radical cation.

Introduction

Recently, the radical cation analogue of the most fundamental electrocyclic ring-opening reaction, i.e., that of the cyclobutene radical cation ($\text{CB}^{\bullet+}$), has been submitted to new theoretical scrutiny by two groups.^{1,2} Thereby, it was found that the reaction leading to the butadiene radical cation ($\text{BD}^{\bullet+}$) occurs via two competitive pathways whose activation enthalpies differ by <1 kcal/mol at the highest level of theory employed in the latter study.² The first of these pathways leads, via a transition state **TS1**, to *cis*- $\text{BD}^{\bullet+}$, following a conrotatory pathway that bears some resemblance to that of the neutral $\text{CB} \rightarrow \text{cis-BD}$ rearrangement but is highly nonsynchronous. The other pathway involves a rotation around the ionized double bond of $\text{CB}^{\bullet+}$ and leads directly to *trans*- $\text{BD}^{\bullet+}$ via a transition state, **TS2**, that shows the characteristics of a cyclopropenylcarbinyl radical cation of the type that had originally been proposed as an intermediate in the $\text{CB}^{\bullet+}$ ring opening by Bauld et al.³ Interestingly, the conrotatory stereochemistry of the process is also preserved along this pathway.



In the search for the transition state for this latter reaction, another stationary point showing a very similar molecular and electronic structure was found at slightly higher energy. This turned out to be the transition state **TS3** for the concerted ring opening of the radical cation of bicyclobutane ($\text{BCB}^{\bullet+}$) to *cis*- $\text{BD}^{\bullet+}$. No well-defined pathway linking **TS2** and **TS3** could be located, mainly because both transition states are located on a very flat region of the potential-energy surface, but there is no

doubt that they interconvert readily. Other transition states for interconverting the four $\text{C}_4\text{H}_6^{\bullet+}$ isomers were found to lie either well below (e.g., that for the *cis*- to *trans*- $\text{BD}^{\bullet+}$ rotation)⁴ or well above **TS1–TS3** (e.g., that for the $\text{BCB}^{\bullet+} \rightarrow \text{CB}^{\bullet+}$ rearrangement).

Several experimental studies have been aimed at elucidating the mode and/or the stereochemistry of the $\text{CB}^{\bullet+}$ ring-opening reaction.^{5–7} All of these involved experiments in the condensed phase, and it is very likely that future studies on this question will also be carried out in liquid or frozen solvents. We therefore decided to use some new tools that have recently become available to investigate the effect that a typical solvent might have on the thermochemistry and the kinetic activation parameters of the different $\text{C}_4\text{H}_6^{\bullet+}$ interconversions described above, in particular the two competing modes of $\text{CB}^{\bullet+}$ ring opening.

Computational Method

The variation of the free energy when going from vacuum to solution is composed of the work required to build a cavity in the solvent (cavitation energy, G_{cav}) together with the electrostatic (G_{el}) and nonelectrostatic work ($G_{\text{disp}} + G_{\text{rep}}$), connected with charging the solvent and switching on solute–solvent interactions.⁸ To these terms (whose sum is referred to as W_{sol}) we must add the contributions due to the variation of the solute’s partition function when going from vacuum to solution. We have assumed that translational and rotational terms remain unmodified (i.e., that the solute has a very large volume available in solvent and that it can freely rotate), whereas we have explicitly computed the variation of harmonic frequencies. Furthermore, W_{sol} can be computed either at the geometry optimized in vacuo (referred to as $W_{\text{sol}}(0)$) or after reoptimizing the geometry in solution ($W_{\text{sol}}(s)$). Entropies are then computed as derivatives of free energies with regard to temperature at constant pressure. The result for the term involving the partition functions is well-known, whereas the derivative of W_{sol} is given by

$$\Delta S_{\text{sol}} = - \left[\frac{\partial (dW_{\text{sol}})}{\partial T} \right] = - \left[\frac{\partial W_{\text{sol}}}{\partial \epsilon} \right] \left[\frac{\partial \epsilon}{\partial T} \right] - \left[\frac{\partial (dW_{\text{sol}})}{\partial V} \right] \left[\frac{\partial V}{\partial T} \right]$$

ϵ and V being the dielectric constant and the volume, respectively.

[†] Università Federico II.

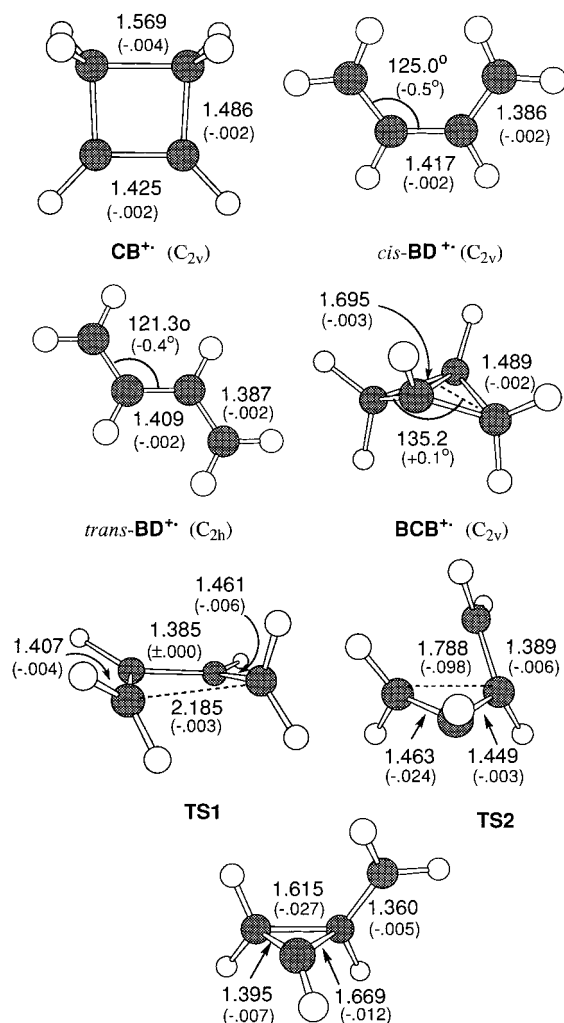
[‡] University of Fribourg.

[§] Present address: Department of Chemistry, Pondicherry University, Pondicherry 605 014, India.

TABLE 1: Thermodynamic and Kinetic Parameters (at 298 K and 1 atm) Computed at the CCSD(T)/cc-pVTZ//B3LYP/PCM Level in Vacuum and in CHCl₃^a

	ΔH_{vac}^b	ΔS_{vac}^b	ΔG_{vac}^b	$W_{\text{sol}}(0)^c$	$W_{\text{sol}}(s)^d$	ΔH_{sol}^e	ΔS_{sol}^f	ΔG_{sol}^g	$\Delta G_{\text{vac}} + W_{\text{sol}}(0)^c$	$\omega_i(\text{vac})^b$	$\omega_i(\text{sol})^h$
CB^{•+}	0.0	0.0	0.0	-44.3	-44.4	0.0	0.0	0.0	0.0		
TS1	17.4	+0.7	17.2	-40.0	-40.6	20.1	-3.7	21.2	21.2	499	504
<i>cis</i> - BD^{•+}	-17.5	+2.3	-18.2	-36.4	-36.5	-9.6	+1.3	-10.0	-9.6		
TS2	18.2	+4.0	17.0	-42.2	-42.4	18.6	-5.0	20.1	20.3	333	269
<i>trans</i> - BD^{•+}	-21.0	+1.7	-21.5	-36.0	-36.0	-13.5	-1.7	-13.0	-12.7		
TS3	19.1	+0.3	19.0	-41.4	-41.4	21.6	-0.3	21.7	22.0	135	168
BCB^{•+}	-0.4	-2.3	0.3	-37.8	-37.9	5.3	-6.0	7.1	6.9		

^a Energies are in kcal mol⁻¹, entropies in cal K⁻¹ mol⁻¹, and frequencies in cm⁻¹. ^b RCCSD(T)/cc-pVTZ//B3LYP/6-31G* from ref 2. ^c $W_{\text{sol}}(0) = G_{\text{cav}}(0) + G_{\text{disp}}(0) + G_{\text{rep}}(0) + G_{\text{el}}(0)$, where (0) indicates the use of geometries optimized in vacuum. ^d $W_{\text{sol}}(s) = G_{\text{cav}}(s) + G_{\text{disp}}(s) + G_{\text{rep}}(s) + G_{\text{el}}(s) - (E_{\text{vac}}(0) - E_{\text{vac}}(s))$, where (s) indicates the use of geometries optimized in solution. ^e $\Delta H_{\text{sol}} = \Delta G_{\text{sol}} + T\Delta S_{\text{sol}}$. ^f $\Delta S_{\text{sol}} = (\partial(\Delta W_{\text{sol}})/T)_p$, calculated under the assumption that only the dielectric constant and the volume change with the temperature. ^g $\Delta G_{\text{sol}} = \Delta G_{\text{vac}}(0) + G_{\text{cav}}(s) + G_{\text{disp}}(s) + G_{\text{rep}}(s) + G_{\text{el}}(s) - (E_{\text{vac}}(0) - E_{\text{vac}}(s)) + RT \ln(Q_{\text{sol}}/Q_{\text{vac}})$, where Q_{vac} and Q_{sol} are the partition functions in vacuo and in solution computed in the rigid rotor/harmonic oscillator approximation. ^h Frequency of imaginary normal mode of transition states.

**Figure 1.** Geometries of the stationary points obtained in CHCl₃. In parentheses are the changes relative to the geometries of the isolated molecules.

The derivative of ϵ with regard to T and the solvent compressibility are taken from the *Chemical Physics Handbook*,⁹ whereas the derivatives of W_{sol} can be computed either numerically or analytically. Finally, enthalpies are obtained from $\Delta H = \Delta G + T\Delta S$.

All computations were performed at the B3LYP/6-31G* level using a modified version of the Gaussian98 package,¹⁰ which includes analytical first and second derivatives of the energy with regard to geometrical parameters of solvated molecules^{11,12} and analytical first derivatives of the energy with regard to the dielectric constant and the volume,¹³ together with

proper use of molecular symmetry.¹⁴ In particular, geometry optimizations and evaluations of Hessians were performed with the CPCM model,¹⁵ whereas final energies were computed with the DPCM model and a very refined compensation of polarization charges.^{11,16} The calculations were carried out in CHCl₃ and H₂O (only the former results are reported here). The cavities were generated by the UAHF model¹⁶ but with the following modifications:

(a) The scale factor (α) for the electrostatic cavity in CHCl₃ was set to 1.4 instead of 1.2 as in H₂O. This was done to account for the larger size of CHCl₃¹⁷ and lack of size reduction due to H bonding.^{18,19}

(b) The charge contraction of the radius of CH_n groups has been evaluated as discussed previously¹⁶ using an equal charge of 0.25 on each group.

The above-described kind of calculation has been shown to also work very well for radicals.^{20,21} $\Delta W_{\text{sol}}(0)$ was evaluated at the B3LYP/6-31G* geometries of isolated *cis*- and *trans*-**BD^{•+}**, **CB^{•+}**, **BCB^{•+}**, as well as **TS1–TS3** obtained previously.² The same geometries were also employed as starting points for the reoptimizations by the B3LYP/6-31G* method in CHCl₃. Single-point RCCSD(T) calculations²² were carried out at these geometries with Dunning's polarized triple- ζ (cc-pVTZ) basis set²³ using the Molpro program.²⁴

Results and Discussion

Table 1 summarizes the results obtained by the procedures described above. The first three columns of data show the thermodynamic parameters in a vacuum (from the data in ref 2). As expected for charged species, the solvation energies $W_{\text{sol}}(0)$ of radical cations (listed in the fourth column) are considerable, and they vary in fact quite substantially, even between different C₄H₆^{•+} isomers, being the highest for **CB^{•+}** where the charge is strongly localized in the double bond. Reoptimizing the different species in the solvent cavity leads to the values $W_{\text{sol}}(s)$ listed in the adjacent column.

As reported in Figure 1, this reoptimization leads only to minor changes in the geometries, except perhaps for **TS1**, which also shows the largest difference between $W_{\text{sol}}(s)$ and $W_{\text{sol}}(0)$. Recalculating the thermodynamic parameters at these new geometries leads to the entries ΔX_{sol} ($X = H, S$, or G) in columns 6–8 of Table 1. In column 9 we juxtapose ΔG_{sol} to ΔG obtained by adding $W_{\text{sol}}(0)$ to ΔG_{vac} . The latter values are uniformly a bit higher but never by more than 0.4 kcal/mol. Thus, the much simpler calculation of $W_{\text{sol}}(0)$ seems to provide a very reasonable approximation to the full results in this case. Nevertheless, we will refer to the thermodynamic parameters obtained after reoptimization in CHCl₃ in the following discussion.

Due to the stronger solvation of $\text{CB}^{\bullet+}$, all three transition states are destabilized by 3–4 kcal/mol in ΔG relative to $\text{CB}^{\bullet+}$ in CHCl_3 , i.e., the rates of the two rearrangements leading to $\text{BD}^{\bullet+}$ are generally expected to be a bit lower in solution than in the gas phase. However, the effect is more pronounced for **TS1** than for **TS2**. Therefore, in CHCl_3 , the pathway leading directly to *trans*- $\text{BD}^{\bullet+}$ is favored by 1 kcal/mol over the “electrocyclic” one leading to *cis*- $\text{BD}^{\bullet+}$, whereas the two ΔG^\ddagger were almost the same in vacuum. Therefore, it is to be expected that in solution experiments the majority of $\text{CB}^{\bullet+}$ would cross over directly to *trans*- $\text{BD}^{\bullet+}$. However, we wish to recall that the conrotatory stereochemistry of the ring opening is also preserved along this completely nonsynchronous pathway.

It is also interesting to note the change in ΔS on going from vacuum to CHCl_3 . $\text{CB}^{\bullet+}$ has the most negative W_{sol} of all the species considered in this study. Although counterexamples are known, the ΔH_{sol} and ΔS_{sol} terms usually show similar trends because a stronger solute–solvent interaction (enthalpic term) generally reduces the mobility of solvent molecules (entropic term). This explains why the slightly positive ΔS_{vac} nearly all become negative in solution. The effect is most pronounced for **TS2** ($\Delta S_{\text{sol}} - \Delta S_{\text{vac}} = -9 \text{ cal K}^{-1} \text{ mol}^{-1}$); the strong enthalpic preference for this transition state over **TS1** in solution is slightly attenuated by entropy. Conversely, the change in ΔS between vacuum and CHCl_3 is the smallest for **TS3**; it lies now only 0.5 kcal/mol above **TS1** on a free-energy scale. However, the rearrangement to $\text{BCB}^{\bullet+}$ will not be competitive with ring opening in solution because, in contrast to the situation in a vacuum, it is now quite strongly endothermic (and endergonic).

The imaginary frequencies at the transition states (last two columns of Table 1) give some indication of the “rigidity” of these structures and can be also used to obtain a rough estimate of tunneling effects through the Wigner expression of the transmission coefficient $x(T)$ which multiplies the conventional rate constant $k(T)$:

$$k(T) = x(T) \left(\frac{kT}{h} \right) \exp \left(\frac{\Delta G^\ddagger}{RT} \right) \text{ with } x(T) = \frac{1}{24} \left[1 - \left(\frac{h\omega_i}{RT} \right)^2 \right]$$

The imaginary frequencies ω_i show that this effect slightly favors **TS1** over **TS2** and **TS3** and that solvent effects are negligible, with **TS2** again showing the largest modification. Furthermore $1.0 < x(T) < 1.15$, so that tunneling effects can be safely neglected.²¹

Conclusions

We have studied solvent effects on the course of the ring opening of the cyclobutene radical cation ($\text{CB}^{\bullet+}$)² by a new implementation of the polarizable continuum model which allows one, for the first time, to take direct (i.e., the energy shift of critical points on the potential-energy surface at geometries in the vacuum), geometrical (i.e., changes in positions of the critical points), and shape effects (i.e., changes of the harmonic environment of the critical points) into full account. Although in the present context only direct effects seem to play a significant role, they have a decisive effect on the course of the ring opening of the cyclobutene radical cation ($\text{CB}^{\bullet+}$)²: whereas in vacuum the two pathways leading to *cis*- and *trans*-butadiene radical cation ($\text{BD}^{\bullet+}$) should occur with very similar rates ($\Delta G_{\text{vac}}^\ddagger = 17.2$ and 17.0 kcal/mol , respectively), embedding the system in CHCl_3 leads to a clear

preference for the reaction leading directly to *trans*- $\text{BD}^{\bullet+}$, in contrast with expectations for an “electrocyclic” ring opening. Of course, these calculations do not take into account counterion effects, which might be important in experiments where the radical cations are generated by photoinduced electron transfer⁵ where the mechanism of the reaction may be indeed be affected by a proximate anion.

Acknowledgment. This work is part of Project No. 98.01915.CT03 of the Italian National Research Council and Project No. 2000-053568.98 of the Swiss National Science Foundation.

References and Notes

- (1) Wiest, O. *J. Am. Chem. Soc.* **1997**, *119*, 5713.
- (2) Sastry, G. N.; Bally, T.; Hrouda, V.; Carsky, P. *J. Am. Chem. Soc.* **1998**, *120*, 9323.
- (3) Belville, D. J.; Chelsky, R.; Bauld, N. L. *J. Comput. Chem.* **1982**, *3*, 548.
- (4) Note, however, that the activation barrier for this process is nearly 1 eV,² i.e., much higher than in neutral **BD**. Thus, under conditions of efficient excess energy dissipation, no interconversion between the two rotamers of $\text{BD}^{\bullet+}$ is expected to occur, even at room temperature.
- (5) Miyashi, T.; Wakamatsu, K.; Akiya, T.; Kikuchi, K.; Mukai, T. *J. Am. Chem. Soc.* **1987**, *109*, 5270.
- (6) Gerson, F.; Qin, X. Z.; Bally, T.; Aebischer, J. N. *Helv. Chim. Acta* **1988**, *71*, 1069.
- (7) Aebischer, J. N.; Bally, T.; Roth, K.; Haselbach, E.; Gerson, F.; Qin, X. Z. *J. Am. Chem. Soc.* **1989**, *111*, 7909.
- (8) Cossi, M.; Barone, V.; Cammi, R.; Tomasi, J. *Chem. Phys. Lett.* **1996**, *255*, 327.
- (9) *Handbook of Chemistry and Physics*; CRC Press: Cleveland, OH, 1981.
- (10) Frisch, M. J.; Trucks, G. W.; Schlegel, H. B.; Scuseria, G. E.; Robb, M. A.; Cheeseman, J. R.; Zakrzewski, V. G.; Montgomery, J. A.; Stratmann, R. E.; Burant, J. C.; Dapprich, S.; Millam, J. M.; Daniels, A. D.; Kudin, K. N.; Strain, M. C.; Farkas, O.; Tomasi, J.; Barone, V.; Cossi, M.; Cammi, R.; Mennucci, B.; Pommelli, C.; Adamo, C.; Clifford, S.; Ochterski, J.; Petersson, G. A.; Ayala, P. Y.; Cui, Q.; Morokuma, K.; Malick, D. K.; Rabuck, A. D.; Raghavachari, K.; Foresman, J. B.; Cioslowski, J.; Ortiz, J. V.; Stefanov, B. B.; Liu, G.; Liashenko, A.; Piskorz, P.; Komaromi, I.; Gomperts, R.; Martin, R. L.; Fox, D. J.; Keith, T.; Al-Laham, M. A.; Peng, C. Y.; Nanayakkara, A.; Challacombe, M.; Gill, P. M. W.; Johnson, B. G.; Chen, W.; Wong, M. W.; Andres, J. L.; Gonzales, C.; Head-Gordon, M.; Repogle, E. S.; Pople, J. A. *Gaussian 98*, Revision Rev. A5; Gaussian, Inc.: Pittsburgh, PA, 1998.
- (11) Barone, V.; Cossi, M.; Tomasi, J. *J. Comput. Chem.* **1998**, *19*, 404.
- (12) Cossi, M.; Barone, V. *J. Chem. Phys.* **1998**, *109*, 6246.
- (13) Cossi, M.; Barone, V.; Pomelli, C.; Tomasi, J. Manuscript in preparation.
- (14) Scalmani, G.; Barone, V. *Chem. Phys. Lett.* **1999**, in press.
- (15) Cossi, M.; Barone, V. *J. Phys. Chem. A* **1998**, *102*, 1995.
- (16) Barone, V.; Cossi, M.; Tomasi, J. *J. Chem. Phys.* **1997**, *107*, 3210.
- (17) Reliable solvation energies for polar species in organic solvents can only be obtained with scale factors larger than that used for water, see, e.g.; Luque, F.; Bachs, M.; Aleman, C.; Orozco, M. *J. Comput. Chem.* **1996**, *17*, 806.
- (18) Solute–solvent hydrogen bonds (which are absent in CHCl_3) decrease the average distance of the first solvation shell, i.e., the dimensions of the cavity in the solute, see: Marten, B.; Kim, K.; Cortis, C.; Friesner, R.; Murphy, R. B.; Rignalda, M. N.; Sitkoff, D.; Honig, B. *J. Phys. Chem.* **1996**, *100*, 11775.
- (19) Recent work has shown that solvent shifts of physicochemical properties which depend on electrostatic terms are much improved using larger scale factors for organic solvents, see: Rega, N.; Cossi, M.; Barone, V. *J. Chem. Phys.* **1996**, *105*, 11060.
- (20) Rega, N.; Cossi, M.; Barone, V. *J. Am. Chem. Soc.* **1998**, *120*, 5723.
- (21) Arnaud, R.; Bugaud, N.; Vetere, V.; Barone, V. *J. Am. Chem. Soc.* **1998**, *120*, 5733 and references therein.
- (22) Knowles, P. J.; Hampel, C.; Werner, H.-J. *J. Chem. Phys.* **1993**, *99*, 5219.
- (23) Woon, D. E.; Dunning, T. H. *J. Chem. Phys.* **1993**, *98*, 1358.
- (24) MOLPRO is a package of ab initio programs: Werner, H.-J.; Knowles, P. J.; Almlöf, J.; Amos, R. D.; Deegan, M. J. O.; Elbert, S. T.; Hampel, C.; Meyer, W.; Peterson, K.; Pitzer, R.; Stone, A. J.; Taylor, P. R.; Lindh, R. *MOLPRO*, Revision 96.1; 1996.